ACS OMEGA

http://pubs.acs.org/journal/acsodf

Article

One-step Green Fabrication of Antimicrobial Surfaces via In Situ Growth of Copper Oxide Nanoparticles

Furkan Sahin, Nusret Celik, Ahmet Ceylan, Mahmut Ruzi,* and M. Serdar Onses*

Cite This: *ACS Omega* 2022, 7, 26504−26513

Read Online

ACCESS | Metrics & More | Article Recommendations | Supporting Information

ABSTRACT: Microorganisms such as pathogenic bacteria, fungi, and viruses pose a serious threat to human health and society. Surfaces are one of the major pathways for the transmission of infectious diseases. Therefore, imparting antipathogenic properties to these surfaces is significant. Here, we present a rapid, one-step approach for practical fabrication of antimicrobial and antifungal surfaces using an eco-friendly and low-cost reducing agent, the extract of *Cedrus libani*. Copper oxide nanoparticles were grown in situ on the surface of print paper and fabric in the presence of the copper salt and extract, without the use of any additional chemicals. The morphology and composition of the grown nanoparticles were characterized using field emission scanning electron microscopy, energy-dispersive X-ray spectroscopy, X-ray photoelectron spectroscopy, and X-ray diffraction techniques. The analysis revealed that the grown particles consist of mainly spherical CuO nanoparticles with an average size of ∼14 nm and its clusters with an average size of ∼700 nm. The in situ growth process enables strong bonding of the nanoparticles to the surface, resulting in enhanced durability against wear and tear. Moreover, the fabricated surface shows excellent growth inhibition ability and bactericidal activity against both gram-negative and gram-positive bacteria, *Escherichia coli* and *Staphylococcus aureus*, as well as antifungal activity against *Candida albicans*, a common pathogenic fungus. The ability to grow copper oxide nanoparticles on different surfaces paves the way for a range of applications in wound dressings, masks, and protective medical equipment.

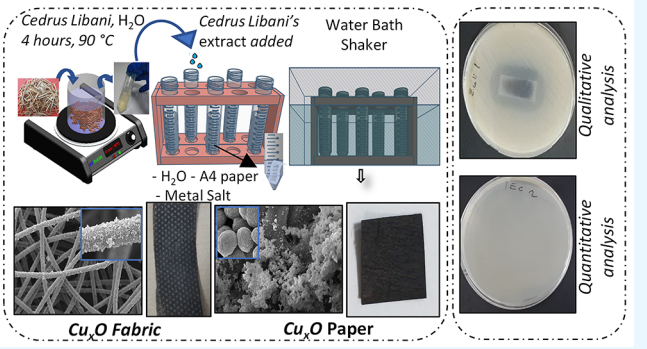

1. INTRODUCTION

Microorganisms like bacteria, fungi, and viruses are part of the ecosystem that humans partake, and from time to time, some of the species can cause serious threat to human life. The COVID-19 pandemic is a recent eminent example. Besides the viruses, some bacteria and fungi species such as *Escherichia coli* and *Staphylococcus aureus* have inflicted a severe toll on humanity for centuries. For example, the Global Action Fund for Fungal Infections estimates that more than 300 million people worldwide are infected with fungal infections every year, while more than 1.5 million die from it.[1,2] Some studies revealed that there is a ∼20% mortality in diseases caused by *E. coli* and *S. aureus*.[3,4] One of the main hotbeds and routes for the survival and transmission of these pathogenic microorganisms are highly touched surfaces such as portable equipment, bank notes, and door knobs.[5−8] Regular disinfection of these surfaces and washing hands are conventional methods to mitigate infection. However, the excessive use of chemicals and water is a serious concern from a sustainability perspective. An effective and environment-friendly approach is incorporating antibacterial and antifungal coatings to the surfaces. In this regard, eco-friendly, flexible, and low-cost antimicrobial surfaces are needed.

Due to prominent toxicity to a wide range of pathogenic bacteria and fungus, availability, and low cost, some metals and their oxides, such as Ag, Cu, and Zn, have been used to treat infections since ancient times.[9−11] Nanoparticles of these materials exhibit enhanced antibacterial activity due to their large surface area, and thus various physical and chemical methods have been developed to fabricate antibacterial metal/oxide nanoparticles.[12,13] However, these conventional methods lead to environmental pollution, which is another worldwide problem and therefore necessitates the development of antibacterial surfaces employing eco-friendly materials and processes. In this aspect, green synthesis based on plants and their extracts to reduce metal salts comes to the rescue due to their wide availability and renewability and the environmental friendliness of waste products.[14,15] Phytochemicals and biological molecules such as natural alkaloids, phenolics, flavonoids, glycosides, terpenoids, enzymes, and amino acids are abundant in plant extract and can act as reducing, capping, and stabilizing

Received: April 23, 2022
Accepted: July 6, 2022
Published: July 18, 2022

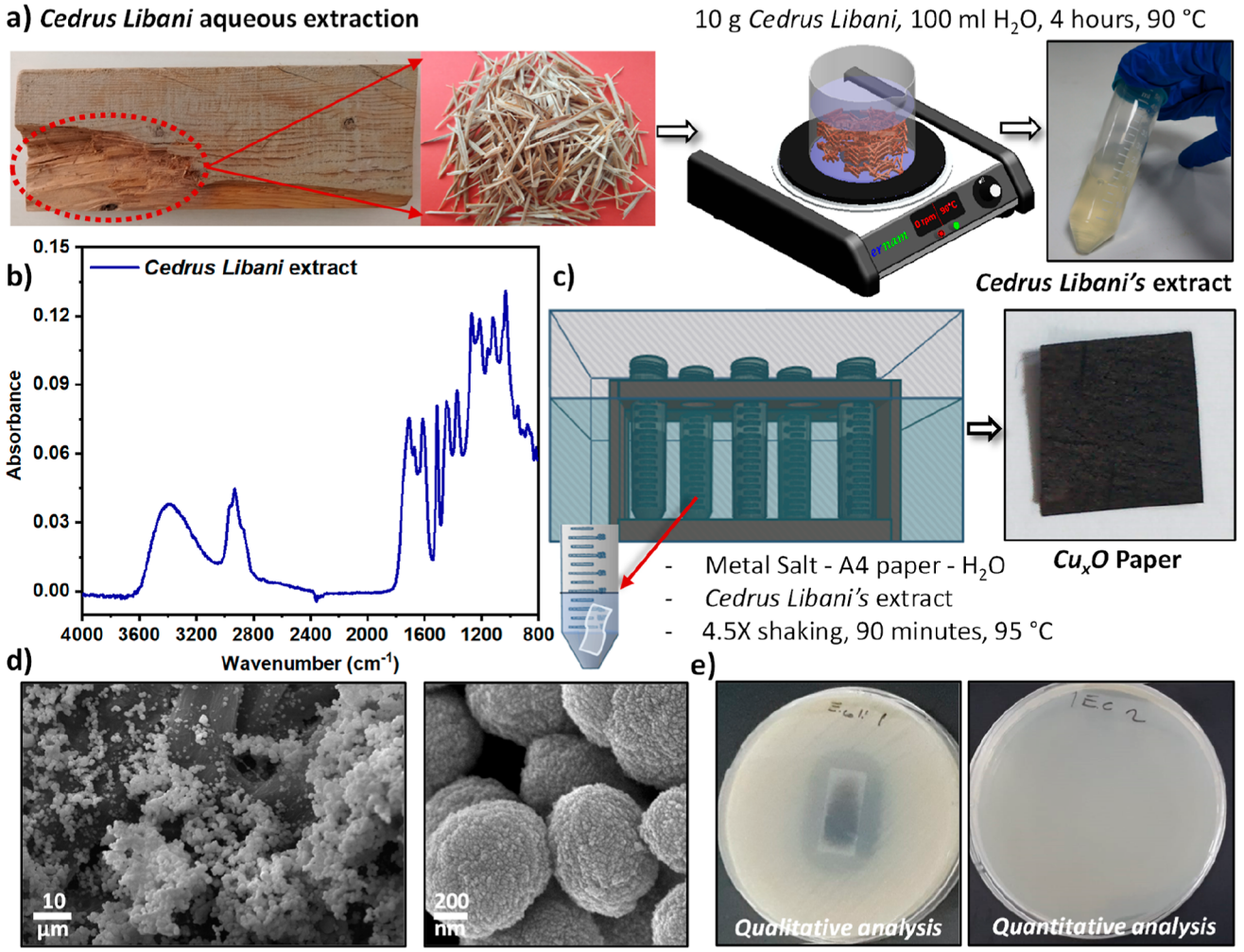

Figure 1. Fabrication and characterization of the antibacterial surface. (a) Photographs of the *C. libani* wood and pieces, an illustration of the extraction process, and a photograph of the extract in a test tube. (b) FTIR−ATR spectrum of the dried extract. (c) Illustration of the reaction setup for reducing the metal salt using the extract under heating and shaking. Also shown is the photograph of the paper after the growth of nanoparticles. (d) FESEM images of the Cu_xO paper surface at different magnifications. (e) Example of the antimicrobial activity of the resultant surfaces against *E. coli*, showing the zone of inhibition against *E. coli* (left) and bactericidal activity (right). No viable bacterial colonies are visible on the agar plate (right).

agents.[16−18] These characteristics allow particles of various shapes and sizes to be fabricated conveniently and with high efficiency.[19,20]

Metallic copper and its oxides are cheap and thus an excellent candidate for fabricating antibacterial surfaces employing green methods, as demonstrated by recent studies.[21−27] Most of these studies follow a similar route: obtaining plant extracts (mostly leaves) and using this extract to reduce metal salts to prepare a colloidal nanoparticle solution, followed by applying these colloidal nanoparticles onto a surface to obtain the final, functional surface. A more direct and robust approach would be to grow the nanoparticles in situ on the desired surface, which can provide a heterogeneous nucleation site to the reduced metal atoms and may reduce the nucleation barrier, thereby enhancing the efficiency. However, there are only a few limited studies on the direct growth of functional nanoparticles on surfaces, mostly on porous materials such as cellulose, cotton, and polyester. Nonetheless, these previous studies demand thermal treatment at high temperatures[22] and usage of corrosive and toxic chemicals[23] and generally require multiple steps.[25] Furthermore, very few studies investigated the robustness of those antipathogenic surfaces, and even those focused only on washing tests related to antibacterial fabrics.[21,28] However, in real-life applications, mechanical abrasion due to touch and scratch are inevitable, and thus the resistance of green fabricated antimicrobial surfaces to abrasion should also be demonstrated.

Herein, we present a practical approach to preparing oxide nanoparticles of copper with very high antimicrobial and antifungal activities in one step using an aqueous extract of *Cedrus libani*, a widely cultivated tree native to the Eastern Mediterranean and is stated to have antibacterial/antifungal ability in folk medicine. The chemical composition and structure of the in situ-grown nanoparticles are characterized, followed by investigating their antibacterial and antifungal activities. The results indicate that the main advantages of the presented approach are the usage of eco-friendly and low-cost materials, which are suited for mass production and mechanical durability.

2. RESULTS AND DISCUSSION

This study presents facile fabrication of antibacterial surfaces using an eco-friendly approach. Specifically, a natural extract from *C. libani* was used for reducing metal salts instead of toxic and expensive chemicals.[29] Furthermore, we also resort to reducing the metal salts on a surface, print paper to be specific.

https://doi.org/10.1021/acsomega.2c02540
ACS Omega 2022, 7, 26504−26513

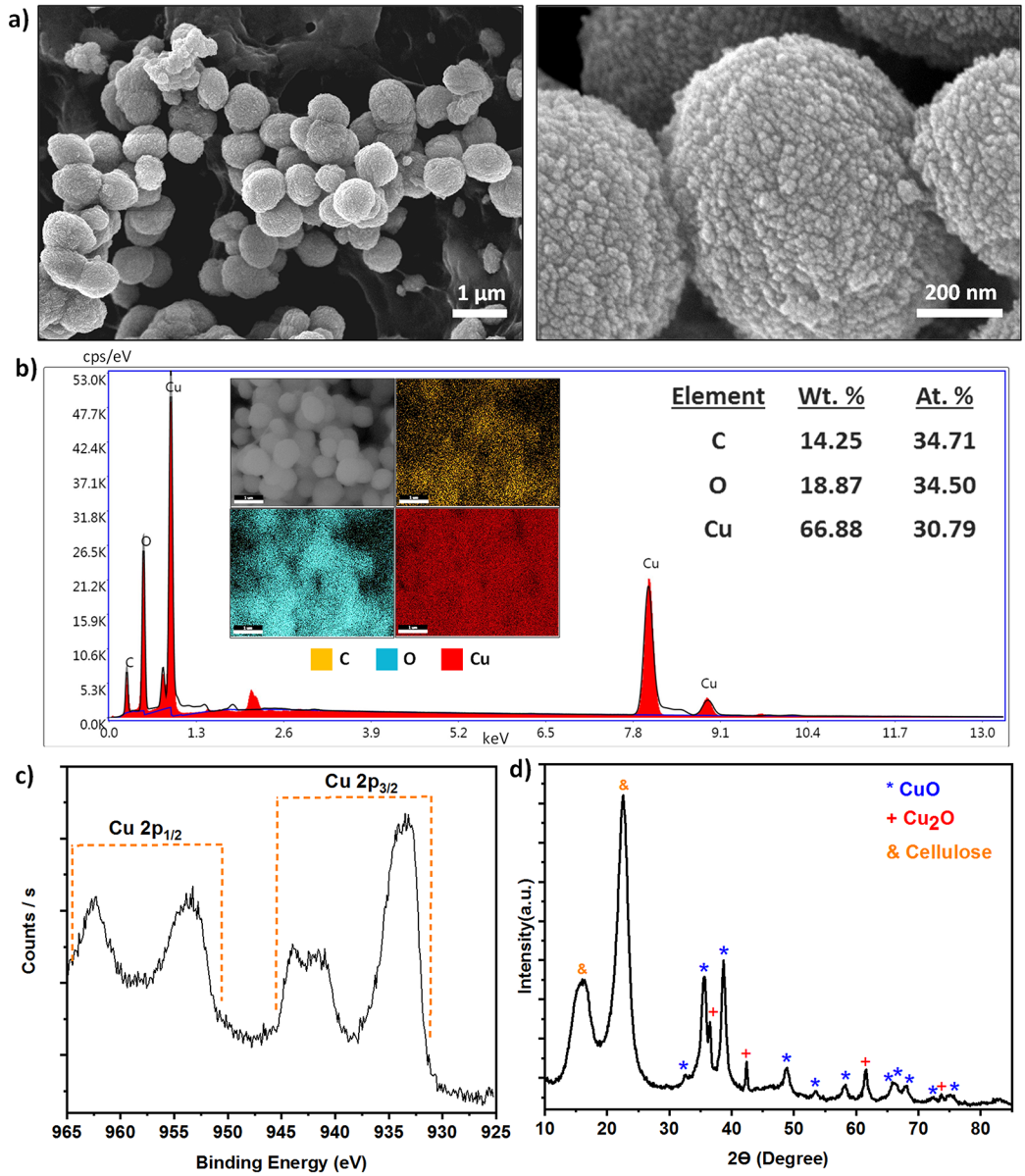

Figure 2. Structural and chemical analyses of Cu_xO paper. (a) FESEM images of Cu_xO paper at the magnification of 10,000 (left) and 100,000 (right). (b) EDX elemental analysis and mapping (inset) of the Cu_xO paper surface. (c) High-resolution XPS spectra of the Cu_xO paper surface around the Cu 2p region. (d) XRD diffraction pattern of the Cu_xO paper surface.

The advantages of growing the nanoparticles on a surface are one-step production, low cost, homogeneity of the surface, and resistance to physical abrasion. Shown in Figure 1a are pictures of *C. libani* and illustrations of the extraction process. Since water is used, only molecules with enough solubility in water are expected in the aqueous extract (pale yellow). The Fourier transform infrared (FTIR) spectrum (Figure 1b) of the dried extract can help shed light on the chemical nature of the components. The strong and broad peak at around 3400 cm^{-1} is due to the O−H stretch vibration and indicates multiple OH groups. The peak at around 2940 cm^{-1} is due to the C−H stretch of alkane groups. The strong and sharp peaks at 1700, 1600, and 1500 cm^{-1} indicate the C═O stretch of carboxylic groups, the C−C stretch of benzene rings, and the bending vibrations of amino groups, respectively. Besides, there are multiple and complex peaks in the fingerprint region due to the C−O stretch and the C−H bending vibrations. Overall, the FTIR spectra suggest the existence of polyphenols and tannins in the aqueous extract, in agreement with previous studies on plant extracts.[30,31] These compounds are known to be able to reduce the metal salts.

The prepared aqueous extract was then mixed with a metal salt in a test tube, and then a piece of paper was immersed into the mixed solution, followed by heating the test tube with a water bath at 95 °C for 90 min. At the end of the reaction, the color of the print paper turns black as a result of the growth of nanoparticles on the surface (Figure 1c). Finally, the antibacterial properties of the surfaces were evaluated by following the protocols of modified ISO 22196 (test for antimicrobial activity) and disk diffusion methods against Gram-positive *S. aureus* and Gram-negative *E. coli* bacteria (Figure 1e).

The structure and morphology of the prepared surfaces were further analyzed using field emission scanning electron

https://doi.org/10.1021/acsomega.2c02540
ACS Omega 2022, 7, 26504−26513

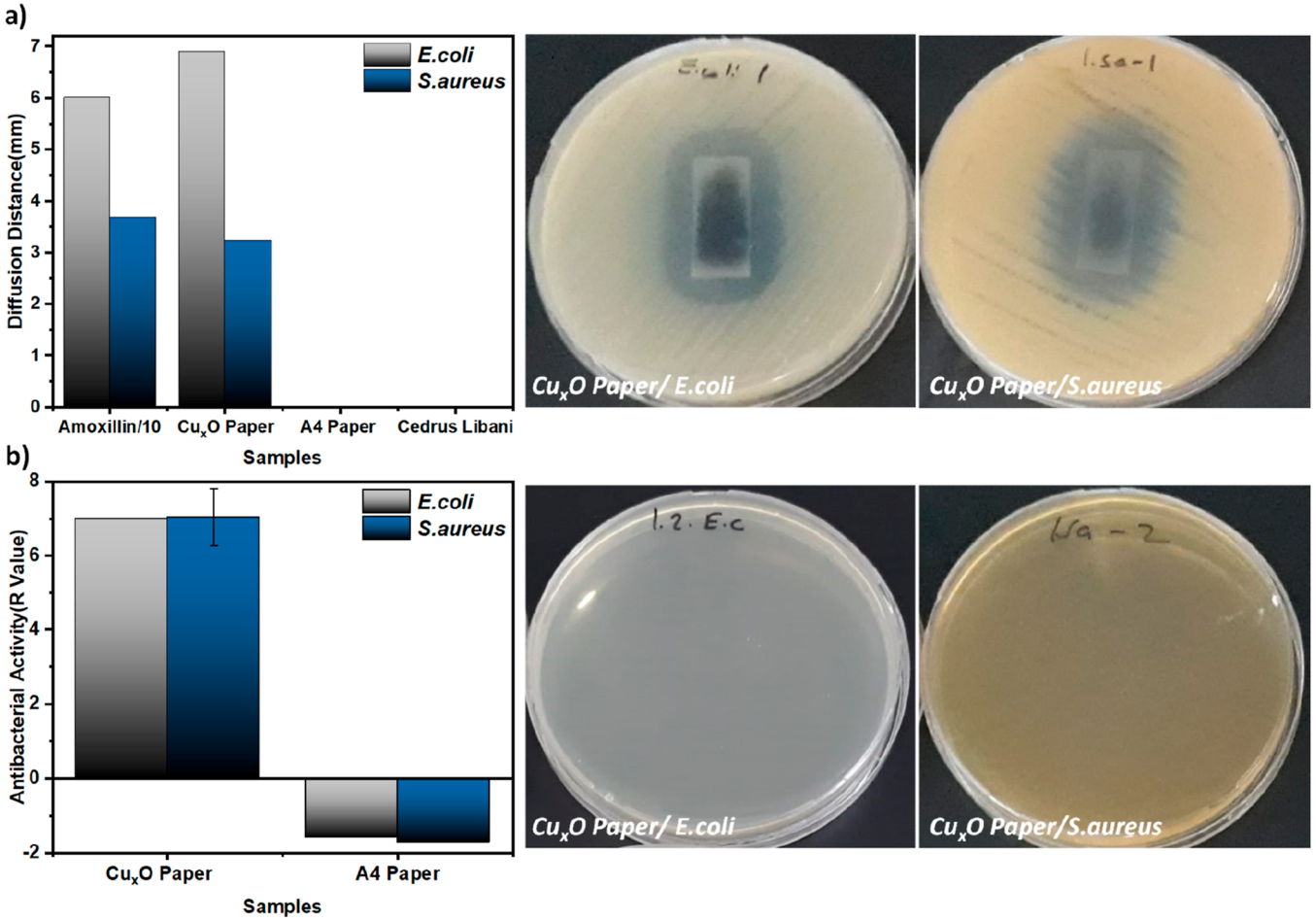

Figure 3. Evaluation of the antibacterial activity of the prepared Cu_xO paper. (a) Bacterial growth inhibition ability of various samples. Left: diffusion distances and right: photographs of agar plate showing the diffusion disk results. (b) Bactericidal activity of the prepared surface. Left: antibacterial activity (*R*-value); right: pictures of agar plate showing killing test for *E. coli* (left) and *S. aureus* (right).

microscopy (FESEM), energy-dispersive X-ray spectroscopy (EDX) mapping, and X-ray diffraction (XRD). Figure 2a shows the FESEM images of the surface, showing that the Cu_xO paper sample surface consists of particles of different scales. The large ones have an average diameter of 0.7 ± 0.1 μm (Supporting Information Figure S1a). On top of the large particles, nanoparticles with an average diameter of 14 ± 4 nm (n = 100) (Supporting Information Figure S1b) are formed. These large particles are likely to be clusters of the primary nanoparticles.

The chemical composition of metallic structures on the surface was investigated by EDX elemental analysis and mapping (Figure 2b). The results show that the ratio of copper atoms to oxygen atoms is close to 1, which indicates the formation of CuO nanoparticles. The EDX mapping suggests a homogeneous surface, which can be explained by the microroughness of the paper providing abundant nucleation sites.[32−34] To better understand the chemical structure of the copper oxide nanoparticles, X-ray photoelectron spectroscopy (XPS) was performed. The XPS survey spectrum consists of characteristics peaks of Cu 2p, O 1s, and C 1s (Supporting Information Figure S2). Furthermore, high-resolution XPS spectra of Cu around the 2p region identifies the chemical state of Cu. A typical XPS spectrum around the Cu 2p region is shown in Figure 2c, where main peaks appear at 933.4 eV (Cu $2p_{3/2}$) and 953.9 eV (Cu $2p_{1/2}$), along with their two shake-up satellites peaks.[35] These satellites show strong configuration interactions and are specific for identifying copper(II).[36] The spectral features of Cu $2p_{1/2}$ and Cu $2p_{3/2}$ peaks (Supporting Information Figure S2a) agree with previous studies.[35−38] However, the peaks seemed to be influenced by copper(I) such as in Cu_2O (Supporting Information Figure S2b,c). In the XPS spectra, the binding energies of Cu(I) and Cu(II) are so close and not differentiable under current experimental conditions, and therefore the surfaces prepared in this study likely contain both species.

To examine the crystal structure of the grown nanoparticles, an XRD analysis was performed. As shown in Figure 2d, the XRD pattern exhibits characteristic peaks at 2θ = 32.6, 35.7, 38.7, 48.8, 53.4, 58.2, 61.6, 65.8, 66.2, 68.1, 72.1, and 75.3° corresponding to the (110), (002, $\overline{1}11$), (111, 200), ($\overline{2}02$), (020), (220), ($\overline{1}13$), (022), ($\overline{3}11$), (220), (311), and (004, $\overline{2}22$) planes of the CuO (JCPDS #no. 05-0661).[39] Additionally, the pattern indicates a crystallized structure due to the peaks observed at 2θ = 36.5, 42.4, 61.6, and 73.7°, which can be assigned to the (111), (200), and (311) crystallographic faces of Cu_2O (reference JCPDS card no. 75-1531).[40,41] As expected, cellulose-specific peaks also appear at 2θ = 15.7 and 22.6°.[42] No other characteristic peaks were observed in the XRD pattern, confirming the high purity of the particles that were synthesized on the surface. Furthermore, the profile of the XRD peak of the CuO nanoparticles due to diffraction from the (111) plane is useful for calculating the primary particle size using the Debye−

https://doi.org/10.1021/acsomega.2c02540
ACS Omega 2022, 7, 26504−26513

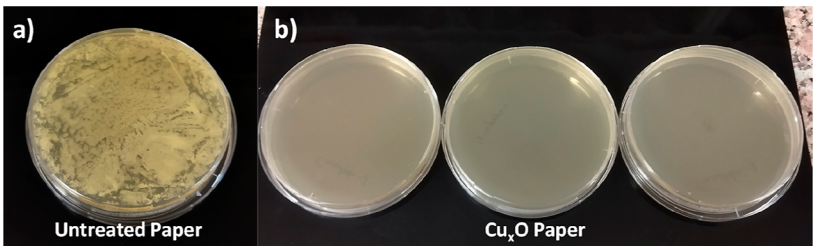

Figure 4. Antifungal activity of Cu_xO paper. (a) Proliferation of *C. albicans* on the untreated paper surface. (b) Agar plate photos showing Cu_xO paper killing all *C. albicans* (n = 3).

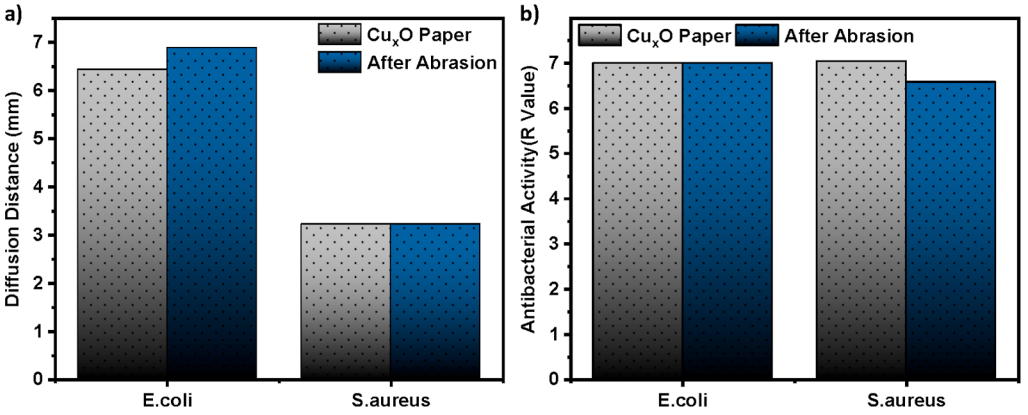

Figure 5. Abrasion resistance of green fabricated antimicrobial Cu_xO paper for practical applications. (a) Change of growth inhibition ability and (b) bactericidal activity of the antibacterial surface before and after abrasion.

Scherrer equation (eq 2). The calculated particle size is 9.8 nm, which is close to the particle size of 14 nm extracted from the FESEM images.

To evaluate the antibacterial activity of the copper oxide nanoparticles grown on the paper surface, two of the most common bacteria, *E. coli* and *S. aureus,* were chosen as test targets. Specifically, the inhibition ability of the fabricated surfaces was assessed qualitatively by calculating the inhibition diameters with the parallel streak method, and the bactericidal activity was evaluated with the modified AATCC 100 method by calculating the kill log rate, as shown in eq 1. As controls, we also evaluated the antimicrobial activity of the print paper and *C. libani* aqueous extract. As shown in Figure 3a, the print paper and *C. libani* aqueous extract did not show any antibacterial activity, while positive control amoxicillin/10 antibiotic showed an inhibition diameter of 6 mm against *E. coli* and approximately 0.4 mm against *S. aureus* (see Supporting Information Figure S3 for more details). On the other hand, the fabricated Cu_xO paper samples showed impressive antibacterial activity with inhibition diameter zones of 6.9 mm against *E. coli* and 3.2 mm against *S. aureus* (Figure 3a). Interestingly, Cu_xO papers exhibited the same antibacterial activity and inhibition diameter even on a small substrate area (1 × 1.5 cm^2) (Supporting Information Figure S4 and Table S1). This may be the result of a dense growth of metallic nanostructures on the surface. Overall, the antibacterial effect of Cu_xO paper can be described as good.[43] These results agree with previous studies where Cu, with the advantages of being oxidized easily, high solubility, and high ion release rate, shows impressive antibacterial activity.[44−46]

To evaluate the antibacterial effect of green-fabricated surfaces quantitatively, a colony of 2.5 × 10^5*E. coli* and 5.6 × 10^5*S. aureus* were cultivated on the surfaces, and the bactericidal efficacy of the surfaces was quantified by colony counting after 24 h of incubation. The fabricated Cu_xO samples showed complete killing for *E. coli* and *S. aureus* (Figure 3b). On the other hand, the microorganisms increased approximately 100-fold on untreated paper, proving that pure paper had no antibacterial activity (Table S2 and Figure S5). The prepared Cu_xO paper is hydrophilic (water contact angle is 34°, see Figure S6) which is beneficial for increasing the contact surface area via facilitating the spreading of the bacterial solution, thus increasing bactericidal activity.

Besides the two common bacteria, *Candida albicans* is a fungal species that causes serious health concerns as it is the leading cause of nosocomial infections, especially among immunocompromised individuals.[47,48] Motivated by this challenge, we examined the antifungal properties of the Cu_xO paper. Figure 4 shows the results of the fungicidal test. The Cu_xO paper substrates completely killed the fungi placed on it (antifungal activity R = 7), while the fungi grew aggressively on the untreated paper sample (control). One of the possible mechanisms of the high antifungal activity of the surface is fungal apoptosis induced by oxidative stress via increasing reactive oxygen species activation of copper oxide particles.[49] Copper oxide particles can also diffuse into the cell via ionic channels and purines, causing leakage of the cytoplasm, deforming the nuclear membrane, and damaging DNA processes.[50] In addition, it is also possible that the nanoscale spherical particles increase the antimicrobial effect due to the increased surface area/volume ratio.

The high antibacterial and antifungal activities of the nanoparticles grown on paper surfaces show great promise for applications in the hygiene and healthcare sectors. To evaluate the feasibility of the surface in practical applications, the fabricated Cu_xO paper surface was abraded, and its antibacterial activity after abrasion was examined. As shown in Figure 5, the

https://doi.org/10.1021/acsomega.2c02540
ACS Omega 2022, 7, 26504−26513

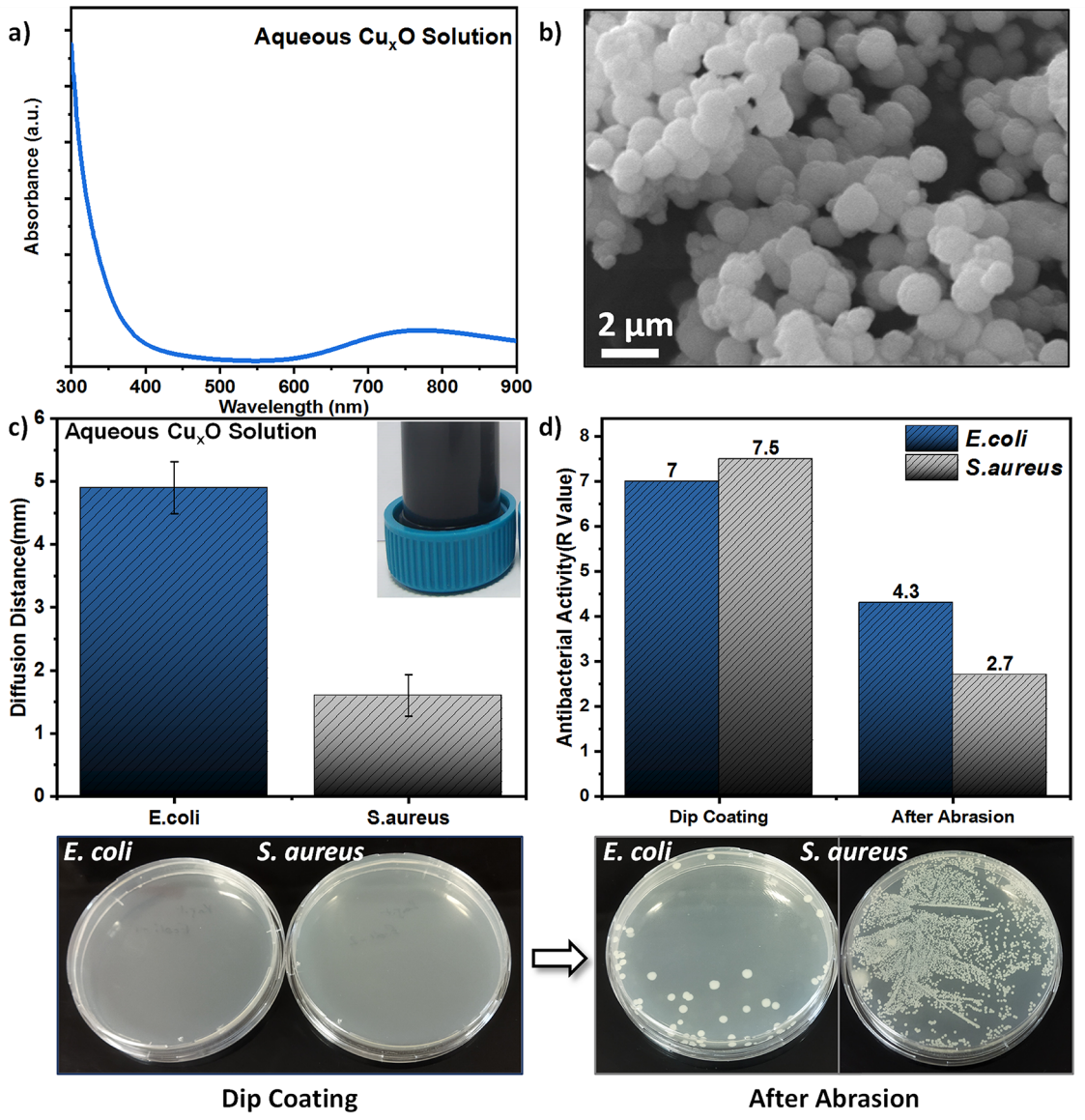

Figure 6. Colloidal synthesis of Cu_xO nanoparticles and evaluation of the antibacterial activity. (a) UV−vis spectra of the Cu_xO nanoparticle solution. (b) SEM images of the print paper after dip coating with Cu_xO nanoparticle solution. (c) Disk diffusion results of green synthesized Cu_xO particles (n = 3). (d) Bactericidal activities of the print paper surface coated with colloidal copper oxide nanoparticles and postabrasion surface (n = 2). The Petri plate photographs show the bactericidal activity of the Cu_xO surface fabricated via dip coating and after abrasion.

average diffusion distance for *E. coli* and *S. aureus* after abrasion was 6.44 and 3.22 mm, while the logarithmic reduction antibacterial activity value was 7 and 6.6, respectively (see details in Supporting Information Figures S7 and S8). This durability test clearly shows that the green fabricated surfaces maintain their antibacterial activity even after mechanical abrasion.

To further investigate the advantage of the in situ growth strategy, we synthesized copper oxide nanoparticles under the same conditions (without paper) and deposited them on the paper surface via dip coating. First, we characterized the synthesized copper oxide nanoparticle solution by measuring the zeta potential (Supporting Information Figure S9) and the UV−vis spectra. As shown in Figure 6a, the UV−vis spectra show absorbance maximum at ∼300 nm which is due to the interband transition in CuO. A weak band is also visible at around 750 nm, which is due to unreacted Cu^{2+} ions.[51] To prepare a sample, the synthesized copper oxide nanoparticles were dip-coated onto a piece of print paper for characterization. The SEM image of the dip-coated paper surface shows spherical particles (Figure 6b) with an average size of 1093 nm (Supporting Information Figure S9b). Furthermore, the antibacterial activity of the synthesized colloidal nanoparticles was evaluated. The disk diffusion test was performed by placing 10 μL of the synthesized aqueous Cu_xO solution onto blank discs, and the bactericidal activity against both bacterial species was thus qualitatively confirmed (Figure 6c and Supporting Information Figure S10). Dip coating reveals that the deposition of the synthesized Cu_xO nanoparticles on the paper surface is not homogenous (Supporting Information Figure S11). Surprisingly, these dip-coated surfaces showed extremely good bactericidal activity. However, the durability of the dip-coated surfaces is weak where the bactericidal activity is significantly decreased after abrasion (Figure 6d).

Most importantly, we anticipate that postabrasion antibacterial stability is an advantage of the in situ growth strategy. This

https://doi.org/10.1021/acsomega.2c02540
ACS Omega 2022, 7, 26504−26513

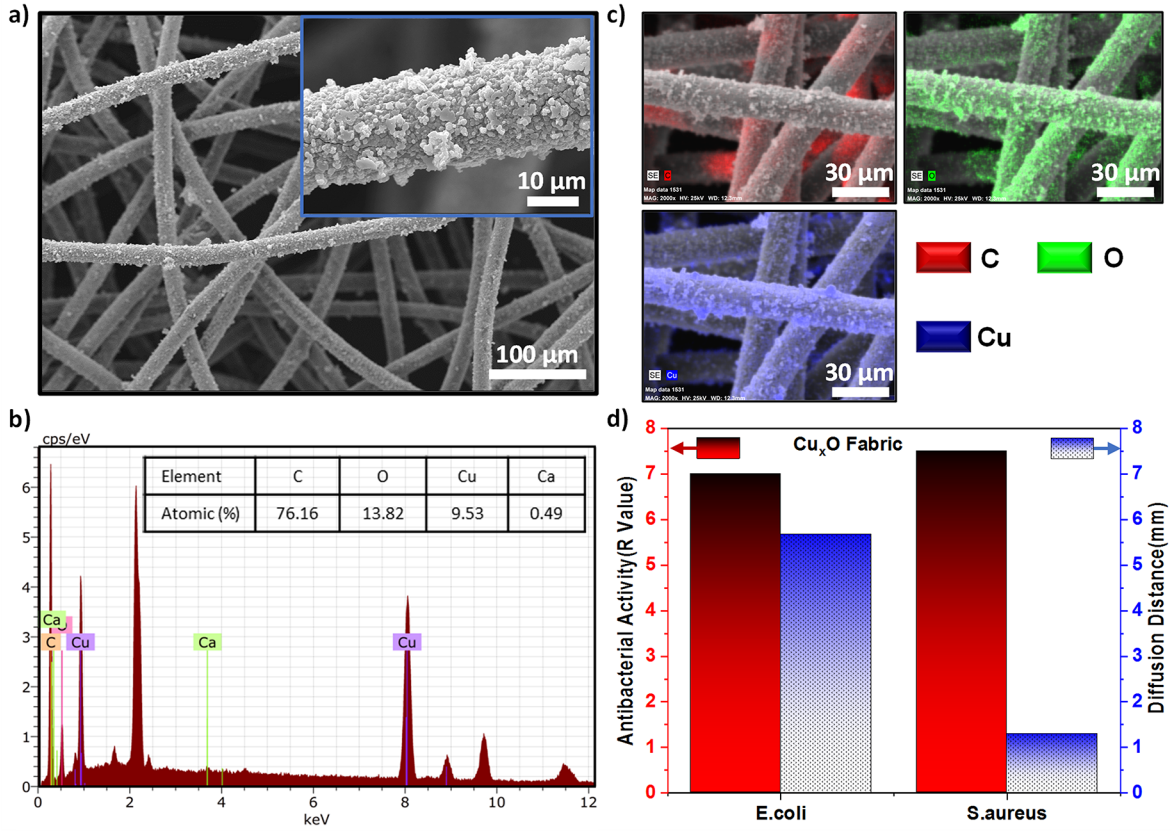

Figure 7. Demonstrating the applicability of the copper oxide particle growth method on different surfaces. (a) SEM images of the Cu_xO fabric surface at 500 magnifications. (b) Elemental mapping of the Cu_xO fabric. (c) EDX elemental analysis of the Cu_xO paper. (d) Qualitative and quantitative antibacterial activities of copper oxide particles grown on the fabric.

makes our surfaces promising for practical applications in the hygiene and healthcare sectors. Encouraged by the strong antibacterial activity and mechanical stability, we have grown the Cu_xO sample on a commercial fabric (used for fabricating masks) under the same conditions to show that it can be used for wound dressing, mask, gauze, and so forth (Figure 7 and Supporting Information Figure S12). The SEM image and EDX elemental mapping of the prepared fabrics presented in Figure 7a,b show that the nanoparticles grow densely on the fibers of the fabric. The fact that the surface contains Cu/O in a ratio of about 1:1, as on the Cu_xO paper surface, is an indication that the nanoparticles are copper oxide (Figure 7c). As a result of this, the Cu_xO fabric showed antibacterial activity against both *E. coli* and *S. aureus*, with zones of inhibition of 5.7 and 1.3 mm in diameter, respectively. As shown in Figure 7d, the green fabricated Cu_xO fabric killed all bacteria on it, while on the untreated fabric, the viability of the bacteria increased approximately 100 times (Supporting Information Figures S13 and S14). Overall, the antibacterial characteristics of the prepared Cu_xO fabric are comparable with those of the recently reported Cu/Zn coated cotton mask fiber.[52] The bactericidal effect on all green fabricated surfaces is probably the result of nano/micro metallic particles that encounter the bacteria, breaking down the bacterial membrane, infiltrating the cell, or damaging the protein/DNA structures.[53,54]

3. CONCLUSIONS

This study demonstrated the practical fabrication of antimicrobial and antifungal surfaces using a plant extract mediated synthesis of Cu_xO nanoparticles. The aqueous extract was prepared from a widely cultivated plant trunk, and chemical analysis revealed the existence of polyphenols which can easily reduce metal salts. Employing the plant extract and metal sources, copper oxide nanoparticles were successfully grown on print paper and fabrics. These textured surfaces not only provide nucleation sites to accelerate the growth of particles but also enhance the binding of the grown particles to the surface, thus increasing durability against mechanical wear. The most important advantage of the in situ growth strategy is that durable antimicrobial surfaces can be fabricated in a single step with low-cost, abundant materials. The growth of copper oxide particles on the surface of the paper and mask fabric imparted these surfaces' high lethality against *C. albicans*, *E. coli*, and *S. aureus* pathogens. The fact that the presented platform can be applied to different surfaces brings flexibility to antimicrobial application areas. Furthermore, green fabricated surfaces showed good stability against mechanical abrasion. This, along with the possibility of eco-friendly, sustainable, and simple production, brings it one step closer to using it in real-life applications.

4. MATERIALS AND METHODS

4.1. Preparation of Aqueous Extract. Kindling wood of *C. Libani* was collected from the Taurus Mountains near Anamur district, Mersin, Turkey. A chunk of the *C. libani* wood was cut into small pieces, and 10 g of the *C. libani* pieces were placed in a beaker, followed by adding 100 mL of double-distilled water. Afterward, the beaker was heated at 90 °C for 4 h and then

https://doi.org/10.1021/acsomega.2c02540
ACS Omega 2022, 7, 26504−26513

cooled to room temperature. Consequently, the solid content was filtered out with the aid of a filter paper (Macherey-Nagel, MN 640 m, diam. 125 mm), resulting in approximately 60 mL of *C. libani* aqueous extract.

4.2. Growth of Metallic Nanostructures on Surfaces. Print paper or fabric (Evony) was cut into small pieces (1 × 3 cm) and placed in a test tube, followed by sequentially adding 15 mL of distilled water, 100 mg of metal salt [$Cu(CO_2CH_3)_2 \cdot H_2O$, Sigma-Aldrich], and 3 mL of aqueous *C. libani* extract. Afterward, the test tube was placed in a water bath (Memmert WNB14) that was kept at 95 °C, and the content was mixed via shaking at 4.5× for 1.5 h. After that, the surfaces on which the metallic nanostructures were grown (paper or fabric) were retrieved and left to dry at room temperature. For brevity, the prepared sample is called Cu_xO paper (copper oxides).

For comparison, Cu_xO colloid nanoparticles were synthesized under the same conditions following the same procedures for dip coating of surfaces; then a piece of paper was fixed to the bottom of a Petri dish and kept in 15 mL of aqueous copper oxide solution for 1.5 h at room temperature.

4.3. Antibacterial Assay. To evaluate the antibacterial activity of the samples, Gram-negative *E. coli* (ATCC25922) and Gram-positive *S. aureus* (ATCT25923) were used. For quantitative analysis, the AATCC 100 test protocol was followed with slight modification. Specifically, 0.5 McFarland suspension of bacteria was prepared in peptone water, followed by adding a broth (Mueller Hinton) in the ratio of 1/9 (bacteria suspension/broth, v/v). Then, 100 μL of the prepared broth mixture was withdrawn and spread on the prepared sample surface. The samples were kept in a 100 mL flask in an incubator (Innova 42, New Brunswick Scientific) at 37 °C and 85% humidity for 24 h. After that, the samples were retrieved and washed in 10 mL of phosphate buffer solution (PBS, pH = 7.4, Sigma-Aldrich) by sonicating for 10 min and vortexing for 1 min. After washing, 100 μL of the bacterial suspension was taken from the flask and spread onto an agar plate kept in the Petri dish. For *E. coli*, nutrient agar (Merck) was used, and for *S. aureus*, tryptic soy agar (Merck) was used. The number of colonies was counted after keeping the Petri dishes in an incubator at 37 °C for 24 h. Since the bacterial colonies in the control samples grew very densely, the bacterial suspension of the control samples was serially diluted 10^2, 10^4, and 10^6 times after washing and then grown in Petri dishes to be able to count the colonies. The antibacterial activity was quantified using *R* values, as calculated according to eq 1

$$\text{antibacterial activity } (R) = \log(Ut/At) \quad (1)$$

Here, *U*t is the average bacterial colony number obtained from control samples, while *A*t is the average bacterial colony number obtained from prepared surfaces.

To qualitatively measure the ability of the prepared surfaces to inhibit the growth of bacteria, the AATCC 147 parallel streak method was followed. Specifically, a cotton swab was dipped once in a 0.5 McFarland bacterial suspension, and then parallel streak cultivation was done so that there was no space on the agar. The inhibition zone diameter was measured after 24 h of incubation. To compare the inhibition effect of the samples, amoxicillin/10 antibiotic was used as a positive control.

4.4. Antifungal Assay. *C. albicans* was used to evaluate the antifungal activity of the samples. The fungal suspension was prepared in Sabouraud-2% dextrose broth (Merck). Then, 100 μL of the prepared suspension was taken and spread on the Cu_xO paper. For comparison, the antifungal activity of untreated paper was also evaluated and used as the control group. The samples were kept in a cabinet at 37 °C and 85% humidity conditions for 36 h. It was then washed in PBS as in the bactericidal test procedure. After washing, 100 μL of the PBS suspension was taken and spread on Sabouraud 4% dextrose agar (Merck). After 24 h of incubation, fungal colonies on agar were counted, and antifungal activity was calculated according to eq 1.

4.5. Robustness of the Antibacterial Surfaces. The robustness of the antimicrobial surfaces was evaluated using an abrasion test. Specifically, as shown in our previous work,[55] the prepared surfaces were placed under 200 g of weight and moved 100 cm against an aluminum foil. The abrasion test simulates wear and erosion of surfaces which may degrade the antibacterial performance. Therefore, antibacterial activity after abrasion was also evaluated following the same procedures as outlined in the previous section.

4.6. Characterization. An FTIR microspectrometer (LUMOS II, Bruker) was used to characterize the *C. libani* extract. Specifically, a few droplets of aqueous extract were placed on a piece of clean aluminum foil and left to dry. Then, FTIR spectra were measured between 680 and 4000 cm^{-1} at a spectral resolution of 4 cm^{-1} and a scan number of 30 using ATR configuration on five different spots, and the average spectrum was presented.

Surface morphology and chemical composition of the prepared surfaces were characterized using SEM (Zeiss EVO LS10), FESEM (Zeiss Gemini 500), and EDS (Bruker) at 25 keV. The size distribution of surface particles was calculated from the SEM images using ImageJ. The wettability of prepared surfaces was evaluated by measuring the static contact angle of a water droplet (10 μL) using a contact angle goniometer (Attension, Theta Lite). XPS was used to analyze the surface composition of the prepared samples using a photoelectron spectrometer (K-alpha, Thermo Scientific) equipped with a monochromatic Al Kα X-ray source (1486.7 eV). Thin-film XRD analyses were performed using a Panalytical Empyrean diffractometer operating at 40 kV and 30 mA using a Cu Kα radiation source. The average size of crystallites was obtained from the XRD data using the Debye−Scherrer eq 2.

$$D = \frac{0.9 \times \lambda}{\beta \times \cos\theta} \quad (2)$$

where θ, λ, and β are the Bragg's angle of the peaks, the wavelength of X-ray radiation, and the angular width value of peaks at full width at half-maximum, respectively.

■ ASSOCIATED CONTENT

Supporting Information

The Supporting Information is available free of charge at https://pubs.acs.org/doi/10.1021/acsomega.2c02540.

Characterization of Cu_xO nanoparticles and full results of bactericidal and bacterial growth inhibition tests (PDF)

■ AUTHOR INFORMATION

Corresponding Authors

Mahmut Ruzi − *Nanotechnology Application and Research Center, ERNAM—Erciyes University, Kayseri 38039, Turkey;* orcid.org/0000-0003-1945-0418; Email: mruzi17@gmail.com

M. Serdar Onses − *Nanotechnology Application and Research Center, ERNAM—Erciyes University, Kayseri 38039, Turkey;*

https://doi.org/10.1021/acsomega.2c02540
ACS Omega 2022, 7, 26504−26513

Department of Materials Science and Engineering, Erciyes University, Kayseri 38039, Turkey; UNAM-Institute of Materials Science and Nanotechnology, Bilkent University, Ankara 06800, Turkey; orcid.org/0000-0001-6898-7700; Email: onses@erciyes.edu.tr

Authors

Furkan Sahin − *Nanotechnology Application and Research Center, ERNAM—Erciyes University, Kayseri 38039, Turkey*

Nusret Celik − *Nanotechnology Application and Research Center, ERNAM—Erciyes University, Kayseri 38039, Turkey; Department of Materials Science and Engineering, Erciyes University, Kayseri 38039, Turkey*

Ahmet Ceylan − *Faculty of Pharmacy, Erciyes University, Kayseri 38039, Turkey*

Complete contact information is available at: https://pubs.acs.org/10.1021/acsomega.2c02540

Notes

The authors declare no competing financial interest.

■ ACKNOWLEDGMENTS

This work was supported by the Research Fund of the Erciyes University (project number FDK-2021-11321). F.S. acknowledges the financial support from the Council of Higher Education of Turkey (100/2000 YÖK Doctoral Scholarship). M.R. acknowledges the funding from the Scientific and Technological Research Council of Turkey (TÜBİTAK) under the Co-funded Brain Circulation Scheme (CoCirculation2).

■ REFERENCES

(1) Rodrigues, M. L.; Nosanchuk, J. D. Fungal Diseases as Neglected Pathogens: A Wake-up Call to Public Health Officials. *PLoS Neglected Trop. Dis.* **2020**, *14*, No. e0007964.

(2) Bongomin, F.; Gago, S.; Oladele, R. O.; Denning, D. W. Global and Multi-National Prevalence of Fungal Diseases-Estimate Precision. *J. Fungi* **2017**, *3*, 57.

(3) Lamagni, T. L.; Potz, N.; Powell, D.; Pebody, R.; Wilson, J.; Duckworth, G. Mortality in patients with meticillin-resistant Staphylococcus aureus bacteraemia, England 2004-2005. *J. Hosp. Infect.* **2011**, *77*, 16−20.

(4) Abernethy, J. K.; Johnson, A. P.; Guy, R.; Hinton, N.; Sheridan, E. A.; Hope, R. J. Thirty Day All-Cause Mortality in Patients with Escherichia Coli Bacteraemia in England. *Clin. Microbiol. Infect.* **2015**, *21*, 251.

(5) Russotto, V.; Cortegiani, A.; Raineri, S. M.; Giarratano, A. Bacterial Contamination of Inanimate Surfaces and Equipment in the Intensive Care Unit. *J. Intensive Care* **2015**, *3*, 54.

(6) Kumar, J.; Eilertson, B.; Cadnum, J. L.; Whitlow, C. S.; Jencson, A. L.; Safdar, N.; Krein, S. L.; Tanner, W. D.; Mayer, J.; Samore, M. H.; Donskey, C. J. Environmental Contamination with Candida Species in Multiple Hospitals Including a Tertiary Care Hospital with a Candida Auris Outbreak. *Pathog. Immun.* **2019**, *4*, 260.

(7) Angelakis, E.; Azhar, E. I.; Bibi, F.; Yasir, M.; Al-Ghamdi, A. K.; Ashshi, A. M.; Elshemi, A. G.; Raoult, D. Paper Money and Coins as Potential Vectors of Transmissible Disease. *Future Microbiol.* **2014**, *9*, 249−261.

(8) Science Brief: SARS-CoV-2 and Surface (Fomite) Transmission for Indoor Community Environments, CDC https://www.cdc.gov/coronavirus/2019-ncov/more/science-and-research/surface-transmission.html (accessed Jan 23, 2022).

(9) Karagoz, S.; Kiremitler, N. B.; Sakir, M.; Salem, S.; Onses, M. S.; Sahmetlioglu, E.; Ceylan, A.; Yilmaz, E. Synthesis of Ag and TiO2 Modified Polycaprolactone Electrospun Nanofibers (PCL/TiO2-Ag NFs) as a Multifunctional Material for SERS, Photocatalysis and Antibacterial Applications. *Ecotoxicol. Environ. Saf.* **2020**, *188*, 109856.

(10) Karagoz, S.; Kiremitler, N.; Sarp, G.; Pekdemir, S.; Salem, S.; Goksu, A. G.; Onses, M.; Sozdutmaz, I.; Sahmetlioglu, E.; Ozkara, E. S.; Ceylan, A.; Yilmaz, E. Antibacterial, Antiviral, and Self-Cleaning Mats with Sensing Capabilities Based on Electrospun Nanofibers Decorated with ZnO Nanorods and Ag Nanoparticles for Protective Clothing Applications. *ACS Appl. Mater. Interfaces* **2021**, *13*, 5678−5690.

(11) Grass, G.; Rensing, C.; Solioz, M. Metallic Copper as an Antimicrobial Surface. *Appl. Environ. Microbiol.* **2011**, *77*, 1541−1547.

(12) Sahin, F.; Celik, N.; Ceylan, A.; Pekdemir, S.; Ruzi, M.; Onses, M. S. Antifouling Superhydrophobic Surfaces with Bactericidal and SERS Activity. *Chem. Eng. J.* **2022**, *431*, 133445.

(13) Akintelu, S. A.; Folorunso, A. S.; Folorunso, F. A.; Oyebamiji, A. K. Green Synthesis of Copper Oxide Nanoparticles for Biomedical Application and Environmental Remediation. *Heliyon* **2020**, *6*, No. e04508.

(14) Faisal, S.; Jan, H.; Shah, S. A.; Shah, S.; Khan, A.; Akbar, M. T.; Rizwan, M.; Jan, F.; Wajidullah; Akhtar, N.; Khattak, A.; Syed, S. Green Synthesis of Zinc Oxide (ZnO) Nanoparticles Using Aqueous Fruit Extracts of Myristica Fragrans: Their Characterizations and Biological and Environmental Applications. *ACS Omega* **2021**, *6*, 9709−9722.

(15) Hemlata; Meena, P. R.; Singh, A. P.; Tejavath, K. K. Biosynthesis of Silver Nanoparticles Using Cucumis Prophetarum Aqueous Leaf Extract and Their Antibacterial and Antiproliferative Activity against Cancer Cell Lines. *ACS Omega* **2020**, *5*, 5520−5528.

(16) Thakkar, K. N.; Mhatre, S. S.; Parikh, R. Y. Biological Synthesis of Metallic Nanoparticles. *Nanomed. Nanotechnol. Biol. Med.* **2010**, *6*, 257−262.

(17) Kharissova, O. V.; Dias, H. V. R.; Kharisov, B. I.; Pérez, B. O.; Pérez, V. M. The greener synthesis of nanoparticles. *Trends Biotechnol.* **2013**, *31*, 240−248.

(18) Ezealisiji, K. M.; Siwe-Noundou, X.; Maduelosi, B.; Nwachukwu, N.; Krause, R. Green synthesis of zinc oxide nanoparticles using Solanum torvum (L) leaf extract and evaluation of the toxicological profile of the ZnO nanoparticles-hydrogel composite in Wistar albino rats. *Int. Nano Lett.* **2019**, *9*, 99−107.

(19) Srikar, S. K.; Giri, D. D.; Pal, D. B.; Mishra, P. K.; Upadhyay, S. N.; Srikar, S. K.; Giri, D. D.; Pal, D. B.; Mishra, P. K.; Upadhyay, S. N. Green Synthesis of Silver Nanoparticles: A Review. *Green Sustain. Chem.* **2016**, *6*, 34−56.

(20) Singh, A.; Gautam, P. K.; Verma, A.; Singh, V.; Shivapriya, P. M.; Shivalkar, S.; Sahoo, A. K.; Samanta, S. K. Green Synthesis of Metallic Nanoparticles as Effective Alternatives to Treat Antibiotics Resistant Bacterial Infections: A Review. *Biotechnol. Rep.* **2020**, *25*, No. e00427.

(21) Montazer, M.; Dastjerdi, M.; Azdaloo, M.; Rad, M. M. Simultaneous Synthesis and Fabrication of Nano Cu2O on Cellulosic Fabric Using Copper Sulfate and Glucose in Alkali Media Producing Safe Bio- and Photoactive Textiles without Color Change. *Cellulose* **2015**, *22*, 4049−4064.

(22) Emam, H. E.; Ahmed, H. B.; Bechtold, T. In-situ deposition of Cu 2 O micro-needles for biologically active textiles and their release properties. *Carbohydr. Polym.* **2017**, *165*, 255−265.

(23) Sedighi, A.; Montazer, M.; Samadi, N. Synthesis of Nano Cu2O on Cotton: Morphological, Physical, Biological and Optical Sensing Characterizations. *Carbohydr. Polym.* **2014**, *110*, 489−498.

(24) Vasantharaj, S.; Sathiyavimal, S.; Saravanan, M.; Senthilkumar, P.; Gnanasekaran, K.; Shanmugavel, M.; Manikandan, E.; Pugazhendhi, A. Synthesis of Ecofriendly Copper Oxide Nanoparticles for Fabrication over Textile Fabrics: Characterization of Antibacterial Activity and Dye Degradation Potential. *J. Photochem. Photobiol., B* **2019**, *191*, 143−149.

(25) Marković, D.; Deeks, C.; Nunney, T.; Radovanović, Ž.; Radoičić, M.; Šaponjić, Z.; Radetić, M. Antibacterial Activity of Cu-Based Nanoparticles Synthesized on the Cotton Fabrics Modified with Polycarboxylic Acids. *Carbohydr. Polym.* **2018**, *200*, 173−182.

(26) Tong, Y.; Liu, Y.; Dong, L.; Zhao, D.; Zhang, J.; Lu, Y.; Shen, D.; Fan, X. Growth of ZnO Nanostructures with Different Morphologies

by Using Hydrothermal Technique. *J. Phys. Chem. B* **2006**, *110*, 20263−20267.
(27) Sathiyavimal, S.; Vasantharaj, S.; Bharathi, D.; Saravanan, M.; Manikandan, E.; Kumar, S. S.; Pugazhendhi, A. Biogenesis of Copper Oxide Nanoparticles (CuONPs) Using Sida Acuta and Their Incorporation over Cotton Fabrics to Prevent the Pathogenicity of Gram Negative and Gram Positive Bacteria. *J. Photochem. Photobiol., B* **2018**, *188*, 126−134.
(28) Bashiri Rezaie, A.; Montazer, M.; Mahmoudi Rad, M. Low Toxic Antibacterial Application with Hydrophobic Properties on Polyester through Facile and Clean Fabrication of Nano Copper with Fatty Acid. *Mater. Sci. Eng., C* **2019**, *97*, 177−187.
(29) Hussain, I.; Singh, N. B.; Singh, A.; Singh, H.; Singh, S. C. Green Synthesis of Nanoparticles and Its Potential Application. *Biotechnol. Lett.* **2016**, *38*, 545−560.
(30) Nieto-Maldonado, A.; Bustos-Guadarrama, S.; Espinoza-Gomez, H.; Flores-López, Z.; Alonso-Nuñez, K.; Cadena-Nava, G.; Cadena-Nava, R. D. Green Synthesis of Copper Nanoparticles Using Different Plant Extracts and Their Antibacterial Activity. *J. Environ. Chem. Eng.* **2022**, *10*, 107130.
(31) Cuong, H. N.; Pansambal, S.; Ghotekar, S.; Oza, R.; Thanh Hai, N. T.; Viet, N. M.; Nguyen, V. H. New Frontiers in the Plant Extract Mediated Biosynthesis of Copper Oxide (CuO) Nanoparticles and Their Potential Applications: A Review. *Environ. Res.* **2022**, *203*, 111858.
(32) Tong, Y.; Liu, Y.; Dong, L.; Zhao, D.; Zhang, J.; Lu, Y.; Shen, D.; Fan, X. Growth of ZnO Nanostructures with Different Morphologies by Using Hydrothermal Technique. *J. Phys. Chem. B* **2006**, *110*, 20263−20267.
(33) Carapeto, A. P.; Ferraria, A. M.; Boufi, S.; Vilar, M. R.; do Rego, A. M. B. Ion Reduction in Metallic Nanoparticles Nucleation and Growth on Cellulose Films: Does Substrate Play a Role? *Cellulose* **2015**, *22*, 173−186.
(34) Sun, Y.; He, K.; Zhang, Z.; Zhou, A.; Duan, H. Real-time electrochemical detection of hydrogen peroxide secretion in live cells by Pt nanoparticles decorated graphene-carbon nanotube hybrid paper electrode. *Biosens. Bioelectron.* **2015**, *68*, 358−364.
(35) Vasquez, R. P. CuO by XPS. *Surf. Sci. Spectra* **2021**, *5*, 262.
(36) Barreca, D.; Gasparotto, A.; Tondello, E. CVD Cu2O and CuO Nanosystems Characterized by XPS. *Surf. Sci. Spectra* **2021**, *14*, 41.
(37) Vasquez, R. P. Cu2O by XPS. *Surf. Sci. Spectra* **1998**, *5*, 257.
(38) Wu, C. K.; Yin, M.; O'Brien, S.; Koberstein, J. T. Quantitative Analysis of Copper Oxide Nanoparticle Composition and Structure by X-Ray Photoelectron Spectroscopy. *Chem. Mater.* **2006**, *18*, 6054−6058.
(39) Hsieh, S.; Lin, P. Y.; Chu, L. Y. Improved Performance of Solution-Phase Surface-Enhanced Raman Scattering at Ag/CuO Nanocomposite Surfaces. *J. Phys. Chem. C* **2014**, *118*, 12500−12505.
(40) Yang, W. Y.; Kim, W. G.; Rhee, S. W. Radio Frequency Sputter Deposition of Single Phase Cuprous Oxide Using Cu2O as a Target Material and Its Resistive Switching Properties. *Thin Solid Films* **2008**, *517*, 967−971.
(41) Aref, A. A.; Xiong, L.; Yan, N.; Abdulkarem, A. M.; Yu, Y. Cu2O Nanorod Thin Films Prepared by CBD Method with CTAB: Substrate Effect, Deposition Mechanism and Photoelectrochemical Properties. *Mater. Chem. Phys.* **2011**, *127*, 433−439.
(42) Trilokesh, C.; Uppuluri, K. B. Isolation and Characterization of Cellulose Nanocrystals from Jackfruit Peel. *Sci. Rep.* **2019**, *9*, 16709.
(43) Pollini, M.; Russo, M.; Licciulli, A.; Sannino, A.; Maffezzoli, A. Characterization of Antibacterial Silver Coated Yarns. *J. Mater. Sci.: Mater. Med.* **2009**, *20*, 2361−2366.
(44) Ellinas, K.; Kefallinou, D.; Stamatakis, K.; Gogolides, E.; Tserepi, A. Is There a Threshold in the Antibacterial Action of Superhydrophobic Surfaces? *ACS Appl. Mater. Interfaces* **2017**, *9*, 39781−39789.
(45) Luo, J.; Hein, C.; Mücklich, F.; Solioz, M. Killing of Bacteria by Copper, Cadmium, and Silver Surfaces Reveals Relevant Physicochemical Parameters. *Biointerphases* **2017**, *12*, 020301.
(46) Hans, M.; Mathews, S.; Mücklich, F.; Solioz, M. Physicochemical Properties of Copper Important for Its Antibacterial Activity and Development of a Unified Model. *Biointerphases* **2015**, *11*, 018902.
(47) Cavalheiro, M.; Teixeira, M. C. Candida Biofilms: Threats, Challenges, and Promising Strategies. *Front. Med.* **2018**, *5*, 28.
(48) Revie, N. M.; Iyer, K. R.; Robbins, N.; Cowen, L. E. Antifungal Drug Resistance: Evolution, Mechanisms and Impact. *Curr. Opin. Microbiol.* **2018**, *45*, 70−76.
(49) Hou, J.; Wang, X.; Hayat, T.; Wang, X. Ecotoxicological Effects and Mechanism of CuO Nanoparticles to Individual Organisms. *Environ. Pollut.* **2017**, *221*, 209−217.
(50) Roopan, S. M.; Devi Priya, D.; Shanavas, S.; Acevedo, R.; Al-Dhabi, N. A.; Arasu, M. V. CuO/C Nanocomposite: Synthesis and Optimization Using Sucrose as Carbon Source and Its Antifungal Activity. *Mater. Sci. Eng., C* **2019**, *101*, 404−414.
(51) Hung, S. C.; Lu, C. C.; Wu, Y. T. An Investigation on Design and Characterization of a Highly Selective LED Optical Sensor for Copper Ions in Aqueous Solutions. *Sensors* **2021**, *21*, 1099.
(52) Zhang, S.; Dong, H.; He, R.; Wang, N.; Zhao, Q.; Yang, L.; Qu, Z.; Sun, L.; Chen, S.; Ma, J.; Li, J. Hydro Electroactive Cu/Zn Coated Cotton Fiber Nonwovens for Antibacterial and Antiviral Applications. *Int. J. Biol. Macromol.* **2022**, *207*, 100−109.
(53) Phan, D. N.; Dorjjugder, N.; Saito, Y.; Khan, M. Q.; Ullah, A.; Bie, X.; Taguchi, G.; Kim, I. S. Antibacterial Mechanisms of Various Copper Species Incorporated in Polymeric Nanofibers against Bacteria. *Mater. Today Commun.* **2020**, *25*, 101377.
(54) Sukumar, S.; Rudrasenan, A.; Padmanabhan Nambiar, D. Green-Synthesized Rice-Shaped Copper Oxide Nanoparticles Using Caesalpinia Bonducella Seed Extract and Their Applications. *ACS Omega* **2020**, *5*, 1040−1051.
(55) Celik, N.; Sahin, F.; Ruzi, M.; Yay, M.; Unal, E.; Onses, M. S. Blood Repellent Superhydrophobic Surfaces Constructed from Nanoparticle-Free and Biocompatible Materials. *Colloids Surf., B* **2021**, *205*, 111864.

https://doi.org/10.1021/acsomega.2c02540
ACS Omega 2022, 7, 26504−26513